Electronic Supporting Information for

On-surface condensation of low-dimensional benzotriazole – copper assemblies.

Federico Grillo[*a], David Batchelor[b], Christian R Larrea[a], Stephen M Francis[a], Paolo Lacovig[c], Neville V Richardson[a]

[a]*EaStCHEM and School of Chemistry, University of St. Andrews, St. Andrews, KY16 9ST, United Kingdom*

[b]*Karlsruhe Institut für Technologie (KIT)- IPS, Hermann-von-Helmholtz-Platz 1, 76344 Eggenstein, Deutschland*

[c]*Elettra – Sinctrotrone Trieste, S.C.p.A., S.S. 14 km 163.5, 34149 Basovizza, Trieste, Italy*

*federico.grillo@st-andrews.ac.uk

Contents:

S1. Additional STM images

Figure SI1: STM image of BTAH adsorbed on ca. 0.2 ML Cu om Au(111) showing adsorption at copper-rich islands and herringbone elbows. Features at herringbone elbows are elongated following close packed directions. White dashed lines are a guide to the herringbone ridges. 75×75 nm^2, 0.7 nA, -1.5 V.
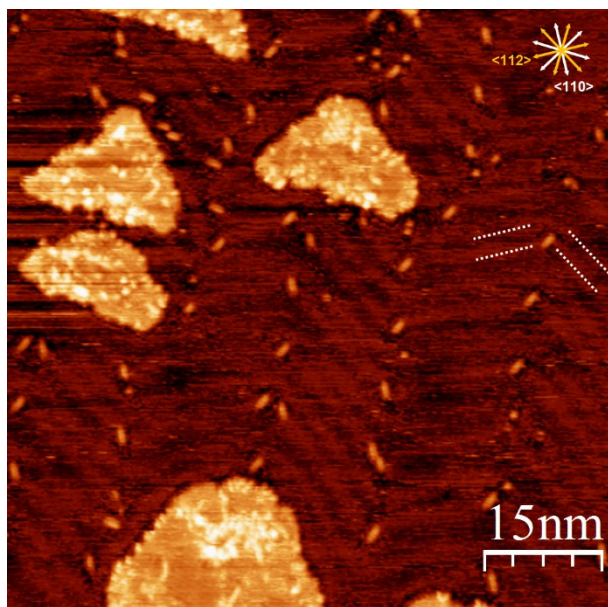

Figure SI2: Features at the steps of copper-rich islands (white arrow) have a width of 0.5 - 0.6 nm. They elongate along a direction normal to the step. These observations indicate that such features may represent single BTA molecules. 25×25 nm^2, 0.3 nA, -1.5 V.
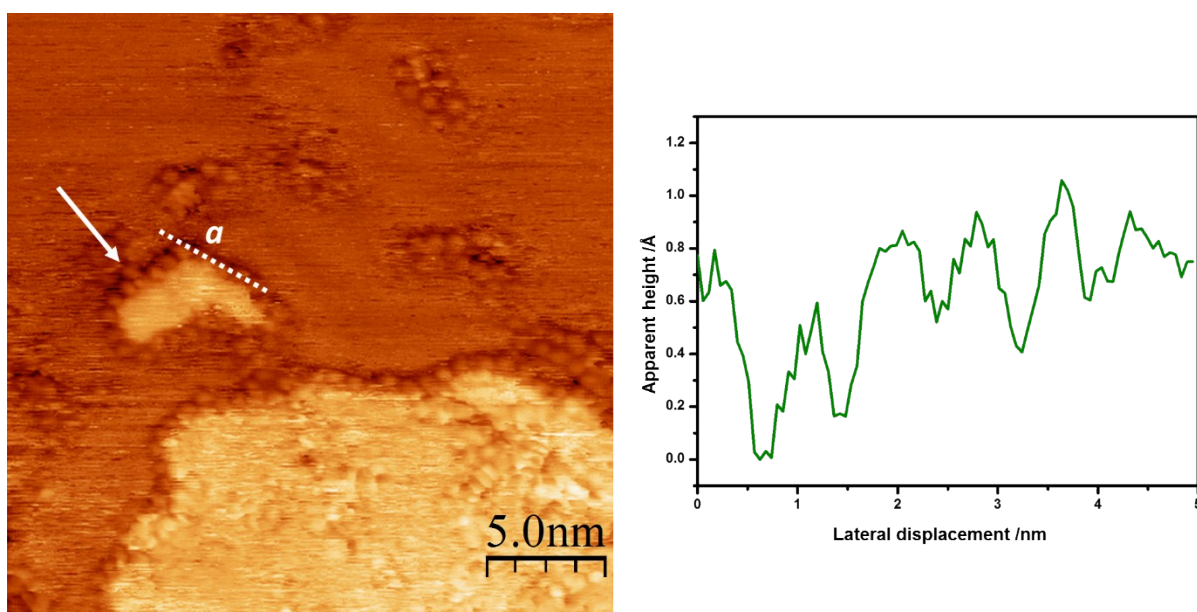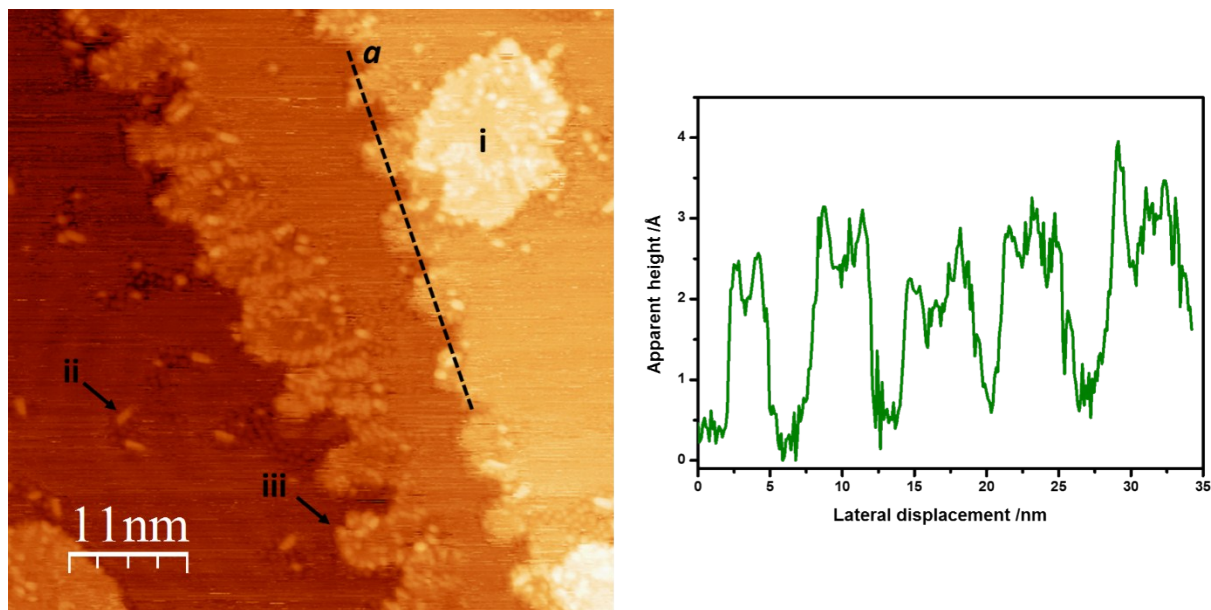
Figure SI3: STM image of BTAH adsorbed on ca. 0.2 ML Cu on Au(111) showing adsorption at copper-rich islands (i), herringbone elbows (ii) and at copper-decorated step edges (iii). The line profile *a* shows an etching spacing of 6.6 - 6.8 nm. 55×55 nm^2, 0.5 nA, -1.5 V.

S2. Additional details on NEXAFS on Au(111)

Figure SI4 shows: a) angular dependent NEXAFS spectra of BTAH dosed to saturation on Au(111) at room temperature; b) 90°-20° spectrum showing opposite dichroism for π* and σ* transitions; c) determination of the average tilt angle of the triazole ring with respect to the surface following the procedure reported in [1 and references therein]; average angle 5° ± 3°; blue lines: interval of confidence; d) comparison between experimental raw spectra collected at 20° and 90° and corresponding calculated spectra for the hydrogen bonded BTAH polymer shown in figure 5e.
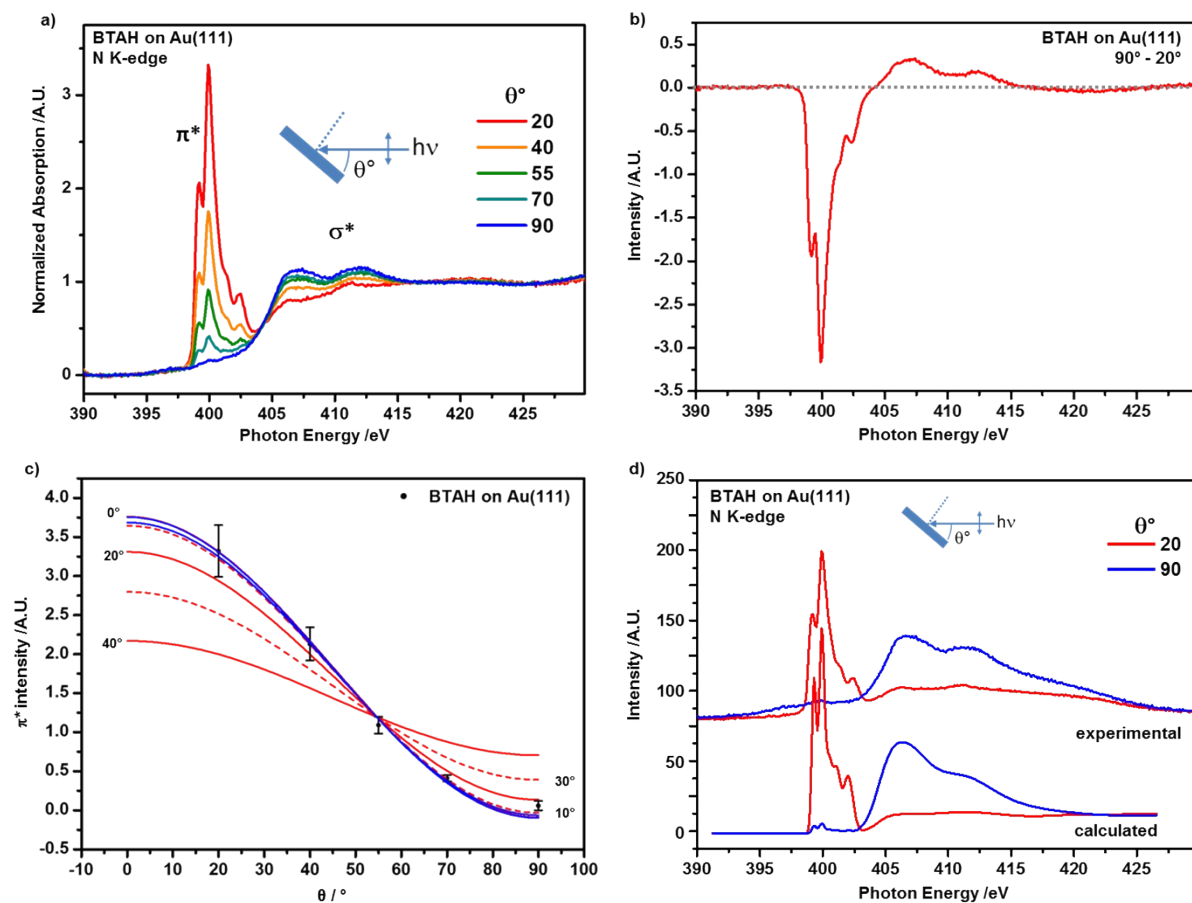
S3. Additional details on NEXAFS on Cu/Au(111)

Figure SI5 show the estimation of average tilt angles of the triazole ring with respect to the surface for BTAH dosed to saturation on 0.2 ML of Cu on Au(111), following the procedure reported in [1 and references therein]: a) as prepared, room temperature; b) after annealing to 400 K; c) after annealing to 500 K; ± 5° interval of confidence in blue.
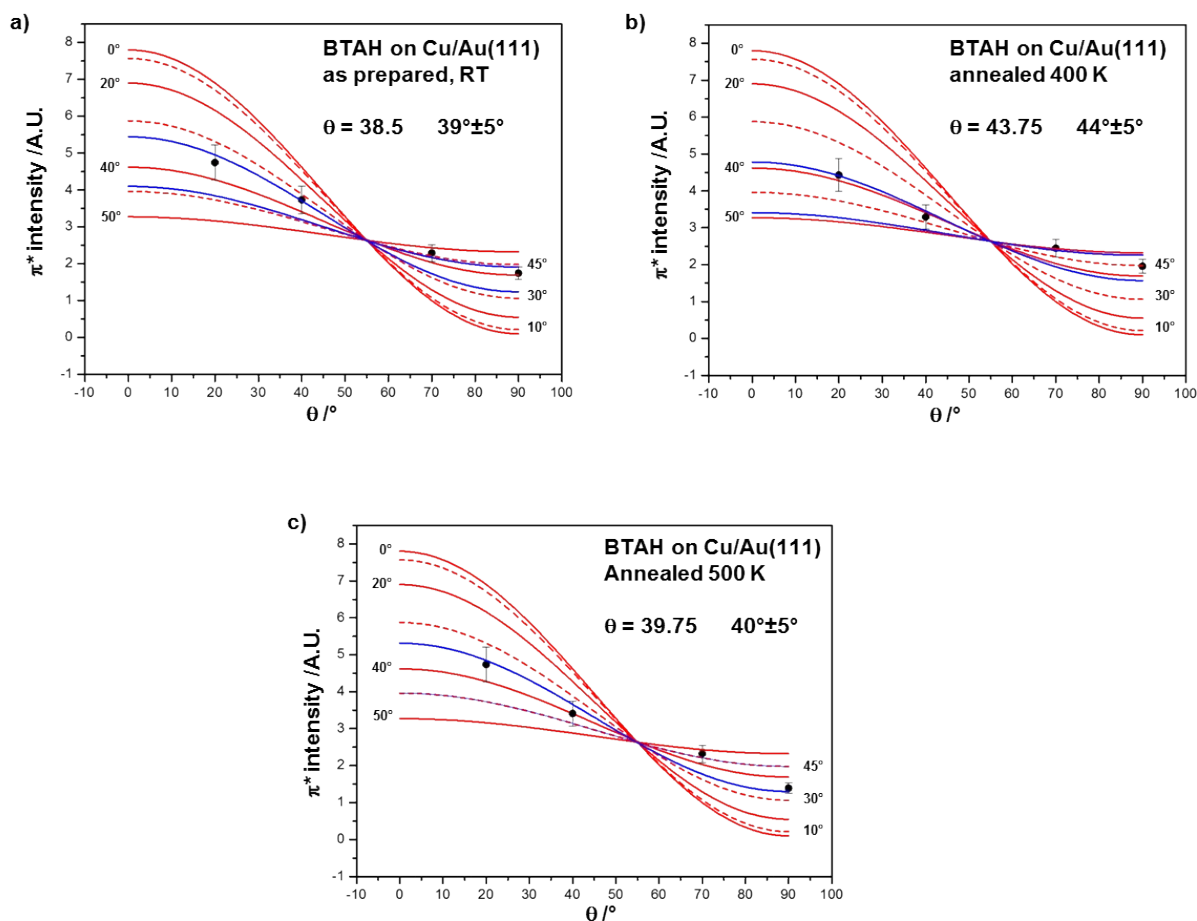
S4. Optimised input geometries for StoBe calculations

The StoBe [2] calculations were performed as described in the manuscript. Molecular species were geometrically optimised; results are reported in the following tables in this section and graphically shown in figures 5e-h. The calculations of the NEXAFS spectra at t N KLL-edge used these geometries, along with the templates in the examples folder included with the StoBe distribution package, following the descriptions in the manuals and StoBe online documentation. The results of the calculations were further processed according to manuals/Internet and [3] to produce the spectra in figure 5a-d. Transitions for the π* systems of the different molecular species are listed in section S5.

Questions regarding these particular calculations and results should be addressed to the co-author david.batchelor@kit.edu.

Other questions concerning the StoBe package should be addressed to the maintainers of the distribution.

H-bonded polymer (figure 5a, 5e)			-[Cu(BTA)]$_n$- polymer (figure 5b, 5f)		
x /Å	y /Å	Atomic number	x /Å	y /Å	Atomic number
0.50	-1.25	7	1.00	0.73	7
0.88	-0.76	7	0.90	-0.06	7
1.00	0.05	7	0.80	0.71	7
0.95	3.75	6	1.03	3.26	6
0.73	2.51	6	0.96	4.44	6
1.04	2.59	6	0.96	2.06	6
0.96	1.37	6	0.84	4.43	6
0.81	1.33	6	0.84	2.05	6
0.80	3.71	6	0.77	3.24	6
0.75	4.66	1	1.13	3.27	1
1.01	4.72	1	1.01	5.40	1
0.61	2.48	1	0.79	5.38	1
1.15	2.62	1	0.67	3.23	1
0.60	-0.79	1	0.65	0.00	29
0.77	0.00	7	0.50	-0.70	7
0.38	-0.44	7	0.40	0.09	7
0.27	-1.21	7	0.30	-0.68	7
0.46	-4.95	6	0.53	-3.23	6
0.23	-3.72	6	0.46	-4.41	6
0.54	-3.78	6	0.46	-2.03	6
0.46	-2.57	6	0.34	-4.40	6
0.31	-2.54	6	0.34	-2.02	6
0.31	-4.92	6	0.27	-3.21	6
0.25	-5.86	1	0.63	-3.24	1
0.51	-5.92	1	0.51	-5.37	1
0.12	-3.70	1	0.29	-5.35	1
0.65	-3.81	1	0.17	-3.20	1
0.10	-0.42	1	0.15	0.03	29
Notes: z = 0 Å link 9.46 Å			Notes: z = 0 Å link 11.15 Å		

Cu(BTA)$_2$ species (figure 5c, 5g)		
x /Å	y /Å	Atomic number
1.83	2.66	7
2.54	1.44	7
3.83	1.66	7
-1.83	2.66	7
-2.54	1.44	7
-3.83	1.66	7
5.21	3.79	6
5.09	5.19	6
2.64	5.07	6
3.83	5.82	6
2.76	3.67	6
4.03	3.04	6
-5.21	3.79	6
-5.09	5.19	6
-2.64	5.07	6
-3.83	5.82	6
-2.76	3.67	6
-4.03	3.04	6
3.77	6.91	1
5.99	5.81	1
1.66	5.56	1
6.19	3.3	1
-3.77	6.91	1
-5.99	5.81	1
-1.66	5.56	1
-6.19	3.3	1
0	2.65	29
Notes: z = 0 Å		

Cu(BTA) -N$_1$- (figure 5d$_1$, 5h)		
x /Å	y /Å	Atomic number
-1.11	-2.50	7
-0.06	-3.28	7
1.10	-2.49	7
-1.43	0.02	6
-0.71	1.21	6
-0.69	-1.18	6
0.71	1.22	6
0.73	-1.16	6
1.45	0.05	6
-2.52	0.00	1
-1.24	2.17	1
1.23	2.19	1
2.55	0.06	1
2.75	-3.26	29
Notes: z = 0 Å		

Cu(BTA) -N$_2$- (figure 5d$_2$, 5h)		
x /Å	y /Å	Atomic number
-1.15	-2.51	7
0.00	-3.22	7
1.15	-2.51	7
-1.44	0.00	6
-0.71	1.18	6
-0.71	-1.21	6
0.73	1.17	6
0.72	-1.22	6
1.45	-0.00	6
-2.53	0.00	1
-1.23	2.14	1
1.25	2.13	1
2.55	-0.01	1
0.00	-5.05	29
Notes: z = 0 Å		

S5. NEXAFS nitrogen excitation energies from StoBe calculations

For the hydrogen bonded polymer (figure 5a, 5e) the first peak (399.9 eV) in the grazing emission spectrum contains contributions from the N_3 atom. The most intense peak at 400.5 eV contains transitions from N_2, with a shoulder at 401.2 eV due to N_1. The peak at 401.6 eV is generated by N_3, whereas that at 402.6 eV has contributions from N_1 and N_2.

For the $-[Cu(BTA)]_n-$ species (figure 5b, 5f), the most intense peak, at 400.4 eV, is generated by $N_{1,3}$, with a shoulder at 400.5 eV due to N_2. The peak at 402.2 eV has contributions from all three nitrogen atoms; whereas the peak at ca. 403.6 eV is generated by N_2.

For the $Cu(BTA)_2$ species (figure 5c, 5g), three peaks are calculated in the $\pi*$ region. The main peak is at 400.3 eV and has contributions from N_2 and N_3; the shoulder at 399.8 eV is attributed to N_1. The broad peak with maximum at 401.5 eV has contributions from all three nitrogen atoms; the peak at ca. 402.2 is generated by N_2 and N_3, and the peak at 403.3 eV is generated by N_3.

For the $Cu(BTA)$ species with copper bound to N_1 (figure $5d_1$, 5h), a complex spectrum is calculated. The peak at 398.8 eV is generated by transitions involving N_1, the peak at 400 eV is generated by N_3, the main peak, at 400.6 eV has contributions form N_1 and N_2, a peak at 401.6 has contributions from N_3, the last peak, with maximum at ca. 402.6 eV has contributions from N_1 and a tail to the higher energy side due to N_2.

For the $Cu(BTA)$ species with copper bound to N_2 (figure $5d_2$, 5h), three peaks in the $\pi*$ region are calculated. The first peak, 399.7 eV is generated by transitions related to $N_{1,3}$ and N_2; the second peak (401.4 eV) has essentially $N_{1,3}$ character, with two shoulders to the high energy side (401.7 and 402.3 eV) bot due to N_2. The peak at 403.5 eV has contributions from $N_{1,3}$.

S6. References

1. M. Cerruti, C. Rhodes, M. Losego, A. Efremenko, J. -P. Maria, D. Fischer, S. Franzen and J. Genzer, Influence of indium–tin oxide surface structure on the ordering and coverage of carboxylic acid and thiol monolayers, Journal of Physics D: Applied Physics, 2007, 40, 4212.
2. StoBe DeMon Density Functional calculations, K. Hermann and L. G. M. Pettersson, M. E. Casida, C. Daul, A. Goursot, A. Koester, E. Proynov, A. St-Amant, D. R. Salahub. Contributing authors: V. Carravetta, H. Duarte, C. Friedrich, N. Godbout, M. Gruber, J. Guan, C. Jamorski, M. Leboeuf, M. Leetmaa, M. Nyberg, S. Patchkovskii, L. Pedocchi, F. Sim, L. Triguero, A. Vela. <http://www.fhi-berlin.mpg.de/KHsoftware/StoBe>.
3. D. R. Batchelor, U. Aygül, U. Dettinger, M. Ivanovic, A. Tournebize, S. Mangold, M. Forster, U. Scherf, H. Peisert and T. Chassé, Insight into the orientation of LBG polymer films by XANES experiment and calculation European Polymer Journal, 2016, 81, 686.